Desalination and Water Treatment
www.deswater.com
doi: 10.1080/19443994.2014.881752

54 (2015) 358–373
April

Taylor & Francis
Taylor & Francis Group

A mechanistic approach to evaluate the effectiveness of red soil as a natural adsorbent for phosphate removal from wastewater

Prangya Ranjan Rout, Puspendu Bhunia*, Rajesh Roshan Dash

Department of Civil Engineering, School of Infrastructure, Indian Institute of Technology Bhubaneswar, Bhubaneswar, Odisha 751 013, India
Tel. +91 674 2306355; Fax: +91 674 2301983; email: pbhunia@iitbbs.ac.in

Received 11 September 2013; Accepted 5 January 2014

ABSTRACT

The present study was conducted to investigate the efficacy of red soil (RS), as a natural adsorbent, for phosphate removal from wastewater. The chemical composition of the adsorbent was determined by proton-induced X-ray emission and proton-induced γ-ray emission methods. Apart from evaluating the influence of major experimental parameters, the equilibrium data were analyzed by different isotherm models and kinetic models. Experimentally obtained values, such as separation factor (R_L), 0.0297, Freundlich exponent (n), 2.994, and Gibb's free energy change (ΔG°), −1.279 kJ mol^{-1}, suggest that the phosphate adsorption by RS was a favorable and spontaneous process. The presence of coexisting anions showed no competing effects on phosphate removal efficiency. For synthetic initial phosphate concentration of 20 mg L^{-1} and contact time of 90 min, phosphate removal efficiency was 96.47% in batch mode and 19 h of breakthrough time in column mode. Whereas with real domestic wastewater having 5.62 mg L^{-1} of initial phosphate concentration, removal efficiency was as high as 99.8% in batch mode and 70 h breakthrough time in column mode. The results of this study suggested that RS can be used as a low-cost and highly efficient adsorbent for phosphate removal from wastewater.

Keywords: Red soil; Phosphate removal; Real domestic wastewater; Adsorption isotherm; Adsorption kinetics

---

1. Introduction

Phosphorus is an important element, extensively contributing towards many biological, agricultural, industrial, environmental, medical, and household applications. Typically, phosphorus exists in the form of organic phosphate (nucleic acid, phospholipids, etc.) and inorganic phosphate (orthophosphate and polyphosphate) [1]. Domestic wastewater being the dominant source contributes more than 45% of total phosphorus load in surface waters [2]. Usually the concentration of phosphorus in domestic wastewater varies in the range of 3–15 mg L^{-1}, out of which approximately 3 mg L^{-1} forms by the breakdown of protein wastes and the remaining comes through the use of detergents [3,4].

Phosphorus usually is the limiting nutrient and sustained inputs of phosphorus (more than 1 mg L^{-1}) to aquatic environments lead to increased rates of eutrophication [3], a widespread problem throughout the world affecting the quality of domestic, industrial,

---

*Corresponding author.

agricultural, and recreational water resources. While phosphorus input from industrial sources can be controlled using any of the known effluent phosphorus removal processes [5] and from agricultural sources, it can be regulated by balance fertilization [6], domestic sources are of the major concern, which needs proper treatment for the removal of phosphorus up to the levels that can be acceptable by natural systems [7].

So far, various techniques have been developed for the removal of phosphorus from wastewater, which broadly classified as physical [8], biological [9], and chemical methods [10]. Physical methods like electrodialysis and reverse osmosis have been proved to be too expensive and inefficient removing only 10% of the total phosphorus [10]. To overcome this problem, biological treatment came into the picture. Biological removal with Phosphorus Accumulating Organisms and Denitrifying Phosphorus removing Bacteria can remove up to 97% of total phosphorus. However, the complex nature of conventional biological phosphorus removal process makes the implementation of this process difficult for wastewater treatment [9]. Similarly, phosphorus removal through the dosing of chemicals such, as iron salts, aluminum, or calcium, is a common method used effectively to reduce effluent concentrations of nutrients released to surface waters. But the chemicals are expensive and their handling and storage is too dangerous, and the method results in higher production of sludge, thus significantly increasing the operational and maintenance cost [2]. As a consequence, the removal of phosphorus compounds through the adsorption process on to various low cost and easily available adsorbent materials has been recognized as one of the most important removal mechanisms [11]. Till date, diverse adsorbents like red mud, activated alumina, Fe-, Al-, Mg-, Ca-, and Si-based substrates, fly ash, blast furnace slag, various soils, etc. have been reported as adsorbents for phosphorus removal [12–17].

For phosphorus removal and retention, soil has been widely used in many wastewater treatment systems as an adsorbent and proved to be very effective [18–20]. Thus, using soil as an adsorbent for phosphorus removal sounds promising, moreover, the use of local soil as the adsorbent undoubtedly can be adjudged as one of the cost-effective and environmentally friendly technology [21]. Red soil (RS) is the highest coverage of all soil groups of the state Odisha (India). Presence of excess amounts of oxides of iron imparts red color to the soil. The soils are strongly to moderately acidic with low to medium organic matters and have poor water retention capacity. The soils are deficient in nutrients, have low cation exchange capacity, high phosphate and sulfur adsorption property, and deficient in calcium and magnesium [22]. All these characteristic features contribute to the possibility of RS to be used as a phosphorus adsorbent. RS should not be confused with Laterite, as it differs from Laterite on the basis of certain parameters like color or hue (RS—7.5 YR- 2.5 YR, Laterite—5 YR to redder), base saturation (RS—50–75, Laterite- <35), pH (RS—5–6.5, Lterite—4.5–5), structure (RS- angular or sub angular blocky, Laterite- compact vesicular, or honeycombed), and SiO_2/R_2O_3 ratio (RS- 1.7–1.8, Laterite- <1) [23].

Keeping the above-mentioned facts in view, the main objective of this study was to inspect the use of RS as an adsorbent for the adsorption of phosphorus. Physico-chemical properties of RS along with surface characteristics have also been investigated. Besides, isotherm and kinetic models have been analyzed and presented to envisage the phosphorus sorption characteristics of RS. Though very few literatures have been observed to report phosphorus adsorptive behavior of laterite, so far to the best of our knowledge, no study has been reported to evaluate the phosphorus adsorption potential of RS.

2. Materials and methods

2.1. Adsorbent

RS, which is widespread in the districts like Ganjam, Dhenkanal, Keonjhar, Raygada, and Koraput of the state Odisha was used as an adsorbent in this study. The adsorbent was collected from the Balibagada village area in Ganjam district. The adsorbent was washed several times with distilled water to remove surface adhered particles, soluble materials and to remove the red color of iron, and dried in hot-air oven at 100°C for overnight. Then it was crushed, passed through 48-mesh sieve, and particles less than 0.3 mm size were used in the adsorption study. The properties and average chemical composition of the material are given in Table 1. For the composition analysis of soil samples, highly sensitive multi-component analytical methods like proton induced X-ray emission (PIXE) and proton induced γ-ray emission (PIGE) were used.

2.2. Domestic wastewater

Wastewater samples were collected from the wastewater collection pool of Netaji Subash Enclave, Bhubaneswar, Odisha. The pool receives domestic

Table 1
Properties and compositions of RS

Properties and compositions	RS
Particle size (mm)	<0.3
pH_{zpc}	7.51
BET surface area ($m^2\,g^{-1}$)	25.55
Bulk density ($g\,cm^{-3}$)	2.25
Porosity (%)	47.12
Specific gravity	4.51
Specific yield (%)	15.37
Specific retention (%)	31.75
SiO_2 (%)	52.45–54.3
Fe_2O_3 (%)	24.21–24.73
Al_2O_3 (%)	21.38–22.17
MgO (%)	4.85–5.01
Na_2O (%)	0.46–0.49
CaO (%)	0.31–0.34

wastewater discharge of around 300 families residing in the residential complex. The general wastewater characteristics such as chemical oxygen demand (COD), biochemical oxygen demand (BOD), total dissolved solids (TDS), ammoniacal nitrogen (NH_4^+-N), nitrate nitrogen (NO_3^--N), total phosphate (PO_4^{3-}-P), dissolved oxygen (DO), and pH were determined, respectively, by colorimetric method (5220-D), 5-Day BOD method (5210-B), method 2540-C, Ion Selective Electrode (ISE) method, 4500-NH_3, 4500-NO_3^-, vanado-molybdo phosphoric acid method (4500-P), Orion 5-Star DO probe, and HACH digital pH meter as per the procedure mentioned in the standard methods for the examination of water and wastewater [24]. The results are shown in Table 2.

Synthetic phosphate stock solution of 1,000 $mg\,L^{-1}$ was prepared by dissolving defined amount of analytical grade anhydrous potassium dihydrogen phosphate (KH_2PO_4) in distilled water. The stock solution was further diluted with distilled water to get the desired concentrations of experimental working solution. Basically, synthetic phosphate solution was used for optimizing different adsorption parameters in both batch and column studies, and the optimized methods were applied to remove phosphate from real domestic wastewater to evaluate and validate the results obtained from synthetic phosphate solution.

Table 2
Characteristics of domestic wastewater

Compositions	Before treatment	After treatment
pH	7.91	7.14
DO ($mg\,L^{-1}$)	2.97	3.30
COD ($mg\,L^{-1}$)	217	173
BOD_5 ($mg\,L^{-1}$)	98	57
TDS ($mg\,L^{-1}$)	360	187
NH_4^+-N ($mg\,L^{-1}$)	17.38	04.38
NO_3^--N ($mg\,L^{-1}$)	2.46	3.17
Total phosphate ($mg\,L^{-1}$)	5.62	0.04

2.3. Analytical methods

PIXE, PIGE were conducted to analyze the mineral composition of the RS. For better resolution and clarity of results, PIXE was done for analysis of elements with atomic number as low as 12 (low Z elements) and PIGE was done for analysis of high Z elements following the method as described by Kennedy et al. [25]. Measurements were carried out using the 2 MeV proton beam obtained from 3 MV Tandem pelletron accelerator.

The adsorbent RS before adsorption and after adsorption, i.e. red soil treated (RST), were characterized by Fourier transferred infra-red spectroscopy (FTIR), X-ray diffraction (XRD), and scanning electron microscopy (SEM). The FTIR spectra were recorded on Bruker ALPHA-FTIR Spectrophotometer. Samples were prepared in KBr disks (2 mg sample in 200 mg KBr). The scanning range was 500–4,000 cm^{-1} and the resolution was 2 cm^{-1} with a scanning rate of 16. The XRD analysis was performed in a X′pert PW 3040/00 (PANalytical) diffractometer at room temperature, with Cu Kα radiation at a scan speed range of $3^\circ\,min^{-1}$, step size of 1 s, 30 kV voltage, and 20 mAmp current. The XRD patterns were recorded in the 2θ range of 20–80°. Surface microstructure and the morphological characteristics of the adsorbent before and after adsorption were evaluated using a scanning electron microscope, SEM, and JOEL JSM-JAPAN with an accelerating voltage of 15 kV and a maximum magnification of 1000X. The specific surface area of RS was determined by the BET nitrogen gas sorption method using a specific surface area analyzer (Gemini2360, Micromeritics, USA).

Phosphate was analyzed by the vanado-molybdo phosphoric acid method, 4500-P according to standard methods for the examination of water and wastewater [24]. Vanadate-molybdate reagent of 1 and 0.5 mL of distilled water were added with 3.5 mL of filtered sample. The mixed solution was analyzed after 10 min with a Perkin–Elmer Lambd-25 UV/VIS spectrophotometer at the detection wavelength of 470 nm. pH_{zpc} of the adsorbent was measured following pH drift method [26].

2.4. Batch study

The batch study was conducted to determine maximum adsorption capacity, adsorption kinetics, and to establish the PO_4^{3-}-P removal pattern using RS as an adsorbent. The effect of contact time, pH, temperature, agitation speed, initial concentrations of phosphate, adsorbent dose, etc. were also investigated. For the determination of the effect of various parameters, a known quantity of adsorbent (0.5–12 g) with 100 mL of the phosphate solution of concentrations varying from 1 to 25 mg L^{-1} were taken in 250 mL Erlenmeyer flasks and agitated at (100–200 rpm) at a temperature range of 15–45°C for a known period of 5–120 min. To determine the effect of contact time on the adsorptive removal of phosphate, the batch studies were conducted for a series of time intervals until equilibrium was achieved. A pre-determined settling period of 1 h was allowed and filtration of supernatant was done using 0.45 μm filter paper, prior to phosphate analysis. The effect of pH on phosphate removal was carried out by adjusting pH of the solution from 2 to12 using 1 M HCl or 1 M NaOH.

2.5. Adsorption isotherm

In order to determine the adsorption isotherm, 6 g of RS was equilibrated with 100 mL phosphate solution of various concentrations (1, 5, 10, 15, 20, 25, 30, 35, 40, 45, and 50 mg L^{-1}) in 250 mL Erlenmeyer flasks for 90 min. The flasks were agitated at 175 rpm in temperature controlled orbital shaker maintained at a temperature of 27 ± 2°C and neutral pH was maintained for the solution. After equilibrium time, the obtained phosphate adsorption data were fitted to the Langmuir and Freundlich isotherm models. Though 50 mg L^{-1} is comparatively higher concentration than that of the concentrations of domestic wastewater (3–15 mg L^{-1}) [3], higher phosphate concentrations are required to establish a good adsorption isotherm.

2.6. Adsorption kinetics

Experiment was performed with 6 g of RS dosed into 250 mL Erlenmeyer flasks containing 100 mL of 20 mg L^{-1}phosphate solutions at neutral pH. The contents of the Erlenmeyer flasks were then agitated at 175 rpm and 27 ± 2 °C temperature in an orbital shaker incubator. The samples were withdrawn at the intervals of 5, 10, 15, 20, 30, 40, 50, 60, 90, and 120 min after the start of the reaction and analyzed for residual phosphate concentration in the solution. The obtained results were analyzed as per pseudo-first-order, pseudo-second-order, and intra-particle diffusion kinetic equations to find out the best-fit kinetic model.

2.7. Column study

Column study was intended for the characterization of packing of adsorbent and the behavior of adsorption during flow through the packed adsorbent. Column tests are normally performed for providing more realistic laboratory results, since it has a greater resemblance to the flux conditions in full-scale constructed filters than short-term stirred batch experiments, which can result in overestimation of sorption capacities [27]. A polyacrylic transparent column having inner diameter 4.5 cm and height 50 cm was used for this study. The column was operated in down-flow mode with adsorbents filled to 20 cm of bed heights. A constant superficial inflow velocity of 4.2 mL min^{-1} was maintained with the help of peristaltic pump (miclins VSP-200-2C) in a continuous mode. Periodic monitoring and data collection were carried out at a regular interval of 1 h to obtain the breakthrough and exhaustion pattern for the adsorbent in the column.

3. Results and discussions

3.1. Characterization of adsorbent

The chemical composition of the RS was analyzed by PIXE and PIGE and the major constituents are given in Table 1. PIXE and PIGE are the highly sophisticated experimental techniques used in the precise determination of elemental composition of a material. The percentage composition of the RS found in this work is in agreement with the RS properties reported earlier [23]. The presence of Fe-, Al- and Mg-oxides are known to play an important role in phosphate removal [28]. Though, the major component of RS was Si-oxide, however; it has a very insignificant role in phosphate removal [29]. Phosphate ions react with Fe- and Al-oxides by ligand exchange forming inner-sphere complexes, whereas the presence of Mg ion facilitates phosphate removal via precipitation and formation of magnesium ammonium phosphate compound, known as struvite [30–32].

FTIR is a simple and reliable technique widely used in both organic and inorganic chemistry, in research, and in industry. It is widely used in quality control and dynamic measurement. The FTIR spectra of the native and phosphorus loaded adsorbent are shown, respectively, in the Fig. 1(a) and (b), which clearly indicates the changes in the functional groups and surface properties of the adsorbent before and after adsorption. The

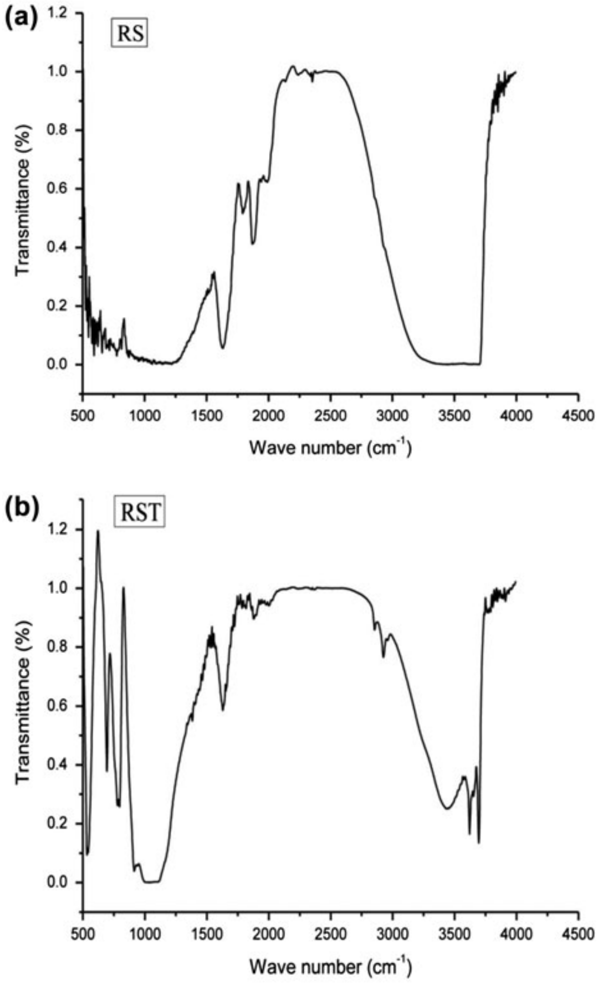

Fig. 1. FTIR spectrum of adsorbent (a) before adsorption; and (b) after adsorption.

FTIR spectrum reveals the complex nature of the adsorbent as evidenced by the presence of a large number of peaks. The infrared absorption between 1,250 and 850 cm^{-1} corresponds to the stretching frequency region of phosphate species [33]. Different peak positions in the above-mentioned range of frequencies again vary depending upon the species of the phosphate ion and probable mineral phase of the adsorbent participating in the adsorption process.

The absorption peak (determined using e-FTIR software) around 1054.23, 1,127, and 1143.45 cm^{-1} in case of RST indicates the participation of P=O entity in adsorption process, which is in agreement with the findings, reported earlier [34]. As a matter of fact, the above-mentioned peaks were not present before phosphorus exposure indicating absence of these functionalities in native adsorbent (RS). There are well-documented experimental results showing that the frequency appearing at 1,126 cm^{-1} is mainly due to adsorption of $H_2PO_4^-$ resulting in P=O stretch [34]. Thus, it can be said that the frequency appearing at 1,127 cm^{-1} in this study is mainly due to the P=O stretch as a result of adsorbed $H_2PO_4^-$. The slight difference in our experimental value and other additional peaks in the frequency ranges may arise due to the presence of different mineral phases within the native adsorbents.

The XRD spectra of adsorbent before and after adsorption are shown in Fig. 2(a) and (b), respectively. There is a visible difference in the diffraction pattern of RS before and after adsorption with respect to shifting of peaks, decrease in intensity of the peaks, and disappearance of peaks. The difference in diffraction pattern of both adsorbents may be the indication of phosphate adsorption. While the peak shift represents the contraction of unit cell, both peak intensity decrease and peak disappearance contributes towards loss of crystallinity of the material under investigation [35].

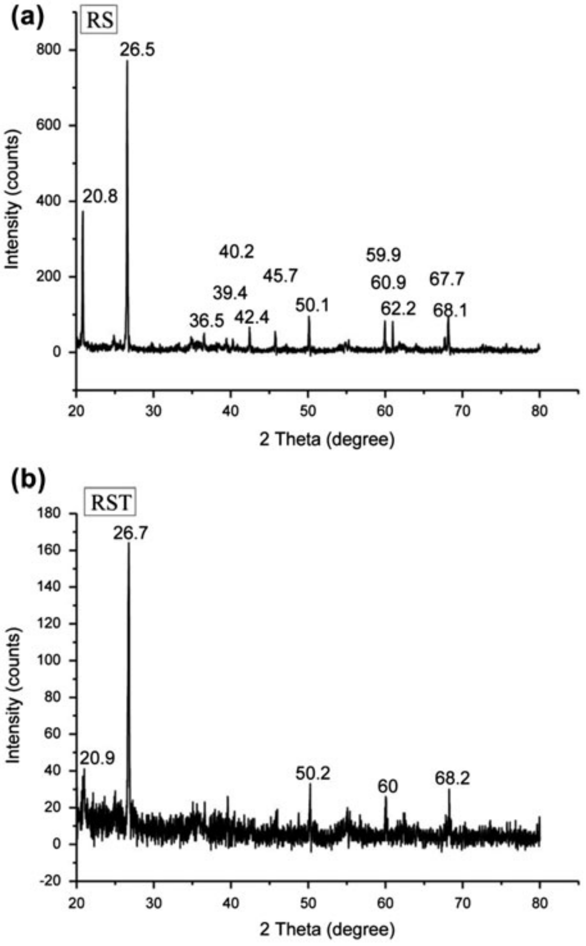

Fig. 2. XRD spectra of adsorbent (a) before adsorption; and (b) after adsorption.

The number of peaks and their respective positions for RS and RST were determined using XPertHighScore software. Comparing Fig. 2(a) and (b), it was found that totally five peaks were common between the diffraction pattern of RS and RST. But in case of RST, the peak intensity reduced drastically with negligible change in peak positions as compared to RS. Also, the number of peaks in 2θ range of 26–50 in the XRD spectrum decreased from seven in case of RS to two in case of RST, making the structure of RST more amorphous than that of RS. This finding suggests the loss of crystallinity due to adsorption of phosphate [36].

The SEM image of the native adsorbent RS is shown in Fig. 3(a). It can be seen from the figure that the presence of irregular grooves and ridges results in a rough and porous surface which is considered suitable for the attachment of phosphate to the adsorbent surface. On the other hand, Fig. 3(b) shows SEM of RST, indicating the presence of fine particles and layer over the surface that are basically absent from the native adsorbent (Fig. 3(a)) before adsorption. This deposition of fine particles and layer is mainly due to the adsorption of phosphates over the surface of RS. The specific surface area and pore volume of the RS were determined to be 25.55 $m^2 g^{-1}$ from the BET analysis. This result is comparable with the findings reported earlier [19,21].

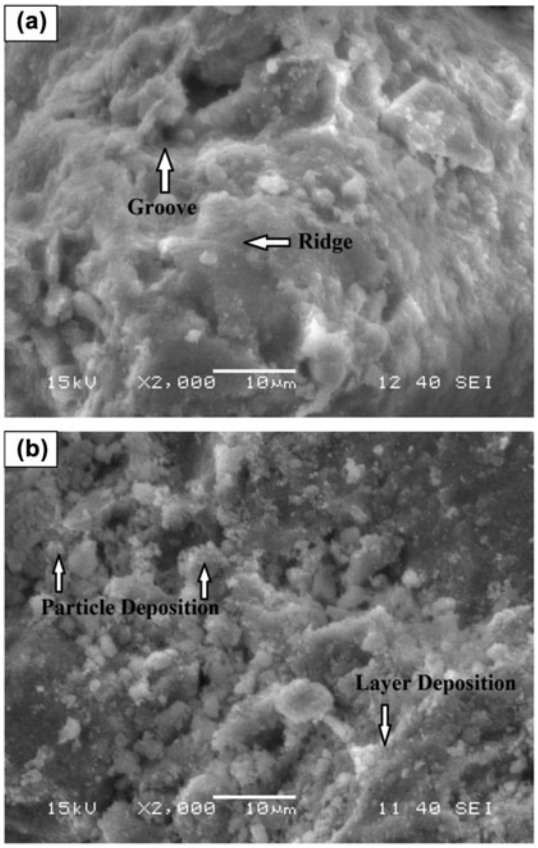

Fig. 3. SEM images of adsorbent at 2000X magnification (a) before adsorption; and (b) after adsorption.

The change in surface properties due to the adsorption of phosphates was evident from the XRD and FTIR results as discussed above. The prominent change in the diffraction pattern of the spent adsorbent to that of the native adsorbent indicates the texture distortion of the adsorbent which may arise due to phosphate adsorption. In order to support the phosphate adsorption by RS, FTIR analysis was also performed. The FTIR spectra of spent adsorbent revealed the presence of peaks corresponding to P=O stretch. Thus, confirming phosphate adsorption. Apart from analyzing the phosphate adsorption with the help of diffraction, absorption, and transmittance properties of the adsorbent, visual observation of phosphate deposition on the adsorbent surface was also conducted by SEM. As observed from Fig. 3(b), SEM enabled the direct visualization of the deposition of fine particles and layers of phosphate on the adsorbent surface. Therefore, adsorption of phosphates by the use of RS as an adsorbent was confirmed by XRD, FTIR, and SEM.

3.2. Batch study

3.2.1. Effect of contact time

The effect of contact time on the adsorption of phosphate by RS was investigated experimentally. The experiments were performed with 100 mL of water containing 20 mg L^{-1} initial phosphate concentration, 6 g of RS, at pH 7, 27 ± 2˚C temperature, and 175 rpm agitation. Elnermayer flasks were removed from shaker after 5, 10, 15, 20, 30, 40, 50, 60, 90, and 120 min and were allowed to settle for 1 h before determining the residual phosphate concentration of the supernatant. The results are shown in Fig. 4. From the figure, contact time of 90 min can be considered as the optimum contact time to reach the equilibrium, resulting in approximately 96% of phosphate removal efficiency. Whereas for 5 min of contact time, this was as low as just 40%. Further increase in contact time over optimum contact time, does not seem to have any significant impact on the equilibrium concentration.

The methods through which adsorbate transfer to the adsorbent include diffusion through the fluid film around the adsorbent particle and diffusion through the pores to the internal adsorption sites. It can also

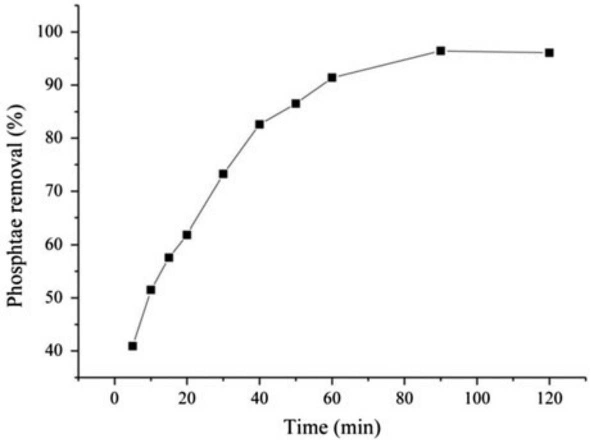

Fig. 4. Effect of contact time on phosphate adsorption. (Conditions: agitation 175 rpm, adsorbent 6 g per 100 mL, adsorbate 20 mg L^{-1}, pH 7, and temperature 27 ± 2˚C).

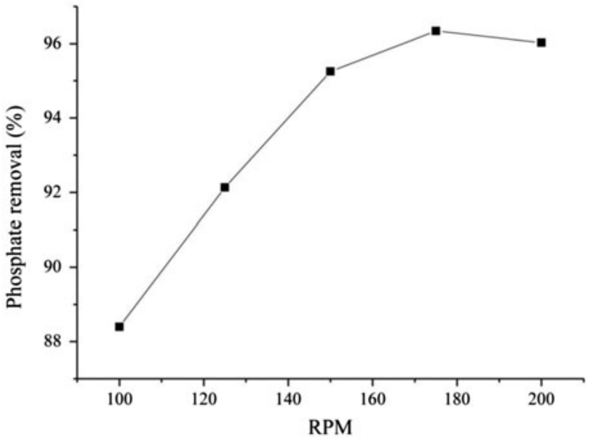

Fig. 5. Effect of agitation on phosphate adsorption. (Conditions: contact time 90 min, adsorbent 6 g per 100 mL, adsorbate 20 mg L^{-1}, pH 7, and temperature 27 ± 2˚C).

be said from Fig. 4 that during the initial phase of adsorption, i.e. up to first 50 min, the slope of the curve is very steep indicating a very fast rate of adsorption (0 to 86.5% removal took place). This can be explained as the maximum surface area of the RS was uncovered while starting the experiment, thus exposing numerous pores and free surface area for adsorption, thereby results in a large concentration gradient between the film and the available pore sites. With the passage of time, more and more surface area and pore sites of the RS get saturated with phosphates. Thus, the available exposed surface of RS decreases, rate of pore diffusion of the phosphates into the bulk of the adsorbent decreases so does the rate of adsorption [37]. This is evident from the figure that only a small amount of phosphate removal takes place during the last 40 min of equilibrium. Therefore, based upon these experiments, the optimum contact time was fixed as 90 min for rest of the experiments.

3.2.2. Effect of agitation

The effect of agitation on phosphate removal was studied at 100, 125, 150, 175, and 200 rpm. The experiments were conducted maintaining the other factors constant such as 20 mg L^{-1} phosphate concentration, 6 g of RS, contact time of 90 min, settling time of 1 h, 27 ± 2˚C temperature, and pH 7. The results are illustrated in Fig. 5. From this, it can be said that the percentage removal of phosphate increases with increase in rotational force, from 88.4% at 100 rpm to approximately 96% at 175 rpm. Increase in rotational speed increases the movement of adsorbent particles in the solution, leading to the reduction of mass transfer boundary. This ultimately improves the surface contact between the adsorbent and the aqueous solution, thereby increasing the rate of phosphate adsorption [38]. But from Fig. 5, it can also be seen that the adsorption rate of RS does not change much beyond 175 rpm, indicating optimum rotational speed as 175 rpm for the adsorption of phosphates by RS.

3.2.3. Effect of adsorbent dose

The effect of adsorbent doses on phosphate adsorption was investigated by varying RS concentration from 0.5 to 12 g per 100 mL of synthetic wastewater containing 20 mg L^{-1} phosphate and maintaining other factors constant such as 90 min of contact time, 1 h of settling time, pH 7, temperature 27 ± 2˚C, and 175 rpm. The results of the study are given in Fig. 6. It can be observed that the phosphate removal efficiency increased from 37.1 to 96.47% by increasing the adsorbent dose from 0.5 to 12 g per 100 mL. The phosphate adsorption rate increases rapidly with the increasing adsorbent concentration due to the availability of more surface area and more adsorption functional sites [20]. Beyond a certain extent, i.e. 6 g per 100 mL in this case, there is no significant uptake of phosphate with an increase in adsorbent dose (Fig. 6). This can be attributed to the attainment of saturation level beyond a certain adsorbent dosage during adsorption process. From Fig. 6, the optimum adsorbent dose of 6 g of RS per 100 mL was fixed for the subsequent experiments. In addition to this, an attempt was made to observe the effect of surface treatment of RS on the sorption behavior of phosphates. RS was activated through acid treatment following a slightly modified method [39].

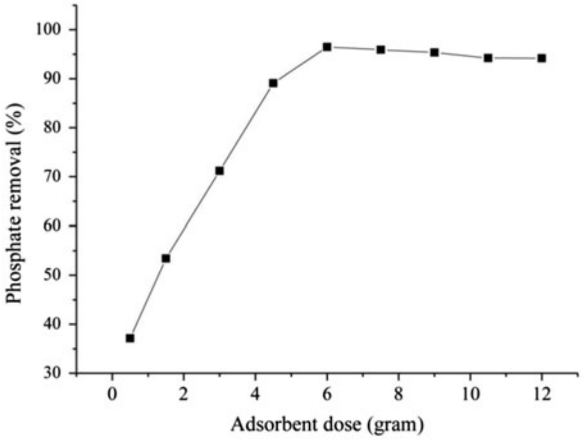

Fig. 6. Effect of adsorbent dose on phosphate adsorption. (Conditions: contact time 90 min, agitation 175 rpm, adsorbate 20 mg L^{-1}, pH 7, and temperature 27 ± 2°C).

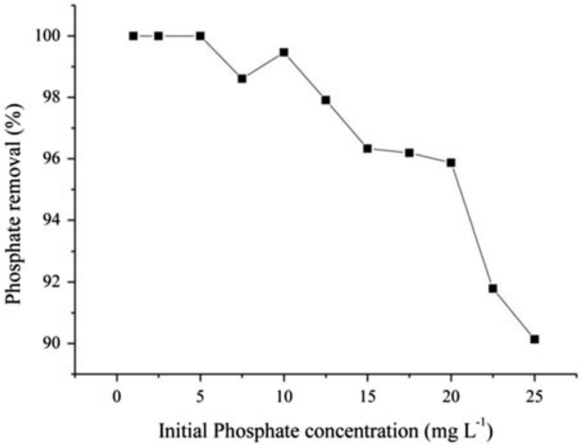

Fig. 7. Effect of initial phosphate concentration on adsorption. (Conditions: contact time 90 min, agitation 175 rpm, adsorbent 6 g per 100 mL, pH 7, and temperature 27 ± 2°C).

The RS was mixed with 0.1 M solution of HCl at a ratio of 1:10 by weight. The mixture was then incubated at 100°C for 12 h. At the end of the treatment, washed thoroughly and oven-dried at 105°C for 12 h, and activated RS was used as an adsorbent. The optimum adsorbent dose in this case was found to be 0.9 g per 100 mL. The high sorption efficiency of the activated RS may be attributed to the increase in active sites and porosity of the material due to acid treatment. This particular study was done only for a comparison purpose. As RS is a natural substance abundantly present in different parts of Odisha, a higher dose of untreated RS can be compromised rather than going for activation of RS by using acid treatment. Therefore, raw RS without any activation was used as adsorbent throughout the study.

3.2.4. Effect of initial phosphate concentration

Iinitial phosphate concentration was varied from 1 to 25 mg L^{-1}in order to evaluate the effect of initial phosphate concentration on the adsorption capacity of the RS (Fig. 7). The experiments were conducted maintaining all the optimized parameters constant. It can be observed that the lower initial concentration of phosphate e.g. 1 mg L^{-1} resulted in higher removal efficiency of approximately 100% as compared to the higher initial concentration of 25 mg L^{-1}, at which removal efficiency was 90.1%. It is evident from Fig. 7 that under lower initial phosphate concentration, adsorption saturation could not be reached due to greater availability of free adsorption sites on the RS as compared to the number of phosphate molecules to be adsorbed, thus resulting in higher phosphate removal efficiency. In case of higher initial phosphate concentration, the available free active adsorption sites on the RS decreases, resulting in lower phosphate removal efficiency (Fig. 7) [3]. The initial phosphate concentration of 20 mg L^{-1} was chosen as the optimum value for the subsequent experiments in order to accommodate maximum possible levels of phosphate in wastewater which are usually in the range of 3–15 mg L^{-1} [3].

3.2.5. Effect of pH

In order to evaluate the effect of pH on phosphate removal, the tests were carried out at pH 2, 5, 7, 10, and 12, maintaining all other parameters constant at their optimum values. It was observed that the maximum phosphate removal efficiency of 97.2% occurred at pH 5 followed by 96.09% at pH 7 (Fig. 8). Phosphate speciation in solution, pH_{zpc} of the adsorbent, the affinity of phosphate ions towards the adsorbent, etc. are the governing factors controlling the effect of pH on phosphate adsorption [36]. There exist three different forms of phosphate, e.g. $H_2PO_4^-$, $H_2PO_4^{2-}$ and PO_4^{3-} in the solution as described in the Eqs. (1)–(3). Normally, $H_2PO_4^{2-}$, and $H_2PO_4^-$ are the predominant species in the pH region between 4 and 10, with $H_2PO_4^{2-}$ being more widespread in slightly alkaline conditions and $H_2PO_4^{2-}$ in slightly acidic conditions. Between pH 10 and 12, $H_2PO_4^{2-}$ dominates over PO_4^{3-} species whereas, at pH higher than 12.5, PO_4^{3-} species are the predominant [40]. pH_{zpc} is the pH at which the net surface charge on the adsorbent is zero. At pH less than pH_{zpc} value, the surface charge of the adsorbent is positive, so a higher Columbic attraction

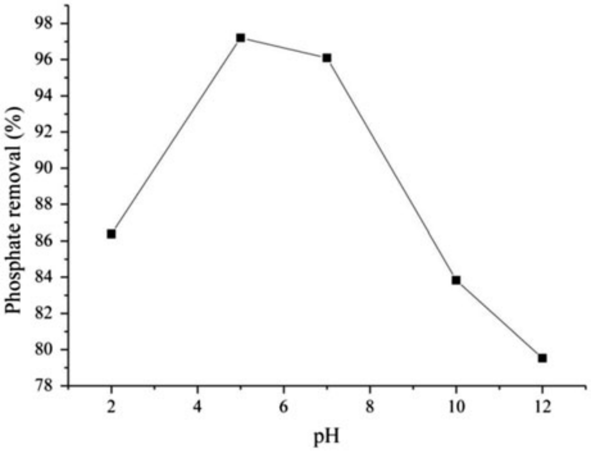

Fig. 8. Effect of pH on phosphate adsorption. (Conditions: contact time 90 min, agitation 175 rpm, adsorbent 6 g per 100 mL, adsorbate 20 mg L^{-1}, and temperature 27 ± 2˚C).

between the binding sites and phosphate ions leads to a higher phosphate uptake. Whereas, at pH greater than pH_{zpc}, the surface has a net negative charge that enhances Columbic repulsion between the sites and the phosphate ions resulting in a decrease in phosphate absorption [41]. The pH_{zpc} of RS was found to be 7.51.

$$H_3PO_4 \leftrightarrow H^+ + H_2PO_4^- \quad pK_a = 2.2 \tag{1}$$

$$H_2PO_4^- \leftrightarrow H^+ + HPO_4^{2-} \quad pK_a = 7.2 \tag{2}$$

$$H_2PO_4^- \leftrightarrow H^+ + PO_4^{3-} \quad pK_a = 12.3 \tag{3}$$

When the solution pH becomes less than pK_a, the solution starts donating more protons than hydroxide groups, making the adsorbent surface positively charged that attracts negatively charged species [42]. In this study, the higher removal of phosphates at pH 5 and 7 indicates that the species involved in adsorption are those which are related to pK_a value of 7.2. In this case, the values of both pHs at which maximum phosphate sorption took place were less than that of (i) pH_{zpc} (7.51) of RS and (ii) pK_a value (7.2) of $H_2PO_4^-$; therefore resulted in the RS surface being positively charged. Thus, based upon this observation, it can be said that $H_2PO_4^-$ was the major species involved in this adsorption process [20,36]. Fig. 8 shows that phosphate removal efficiency at pH 7 (96.09%) is marginally less than that of removal efficiency at pH 5 (97.2%). Therefore, for better convenience neutral pH was set as the optimum pH for subsequent tests.

3.2.6. Effect of temperature

The effect of temperature on the adsorption of phosphate was evaluated by performing the experiments in the temperature ranges from 15 to 45˚C and keeping all other optimized parameters constant (Fig. 9). From Fig. 9, it is observed that the phosphate removal increases from 77.9 to 95.86% with the increase in temperature from 15 to 35˚C. However, there is no further improvement in phosphate removal with the increase in temperature beyond 35˚C. This particular phenomenon can best be described with the help of difference in the types of adsorption, i.e. physical or chemical adsorption. Physical adsorption requires very low activation energy, so the rate of adsorption is high even at low temperature [42]. Therefore, phosphate adsorption onto RS possibly a case of physical adsorption, where 35˚C temperature is enough to achieve the required activation energy for the process to be carried out. An increase in the adsorption process with an increase in temperature up to a certain extent might be due to the diffusional nature of adsorption process which in turn is endothermic in nature [43]. Thus, the temperature beyond 35˚C is not having any major impact on the process. Considering the optimum temperature range (15–35˚C) from the figure, 27 ± 2˚C was adopted as the operating temperature for the further experiments.

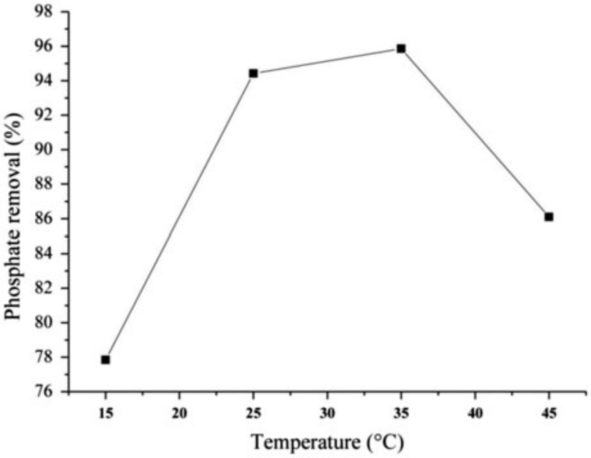

Fig. 9. Effect of temperature on phosphate adsorption. (Conditions: contact time 90 min, agitation 175 rpm, adsorbent 6 g per 100 mL, adsorbate 20 mg L^{-1}, and pH 7).

3.3. Adsorption isotherm

Adsorption isotherms are used to describe the equilibrium relationship between the amount of adsorbate adsorbed $q_e\,(\mathrm{mg\,g^{-1}})$, and the amount of adsorbate in solution $C_e\,(\mathrm{mg\,L^{-1}})$ at constant temperature. The equilibrium uptake capacity q_e can be calculated by using the following equation [44].

$$q_e = (C_0 - C_e)V/m \tag{4}$$

where C_0 and C_e are the initial and equilibrium phosphate concentrations ($\mathrm{mg\,L^{-1}}$), V is the volume of phosphate solution (mL), and m is the mass of adsorbent (g). In this study, Langmuir and Freundlich isotherm models were adopted to fit the equilibrium data obtained from adsorption experiments.

3.3.1. Langmuir model

The Langmuir isotherm suggests monolayer adsorption on a homogeneous surface with a finite number of adsorption sites and without any interaction between the adsorbed molecules [37]. The linearized form of the Langmuir isotherm model is given as:

$$C_e/q_e = 1/(bq_m) + (1/q_m)C_e \tag{5}$$

where q_m is the maximum adsorption capacity ($\mathrm{mg\,g^{-1}}$) and b is adsorption constant ($\mathrm{L\,g^{-1}}$) that measures the affinity of the adsorbent for the solute. The higher value of b suggests a higher level of adsorption. The plot of C_e vs. C_e/q_e as per Eq. (5) is a linear one (Fig. 10(a)) and the values of q_m and b can be obtained considering the slope and intercept of the plot (Table 3). The maximum adsorption capacity (q_m) of RS is found out to be $0.56\,\mathrm{mg\,g^{-1}}$, which is at par with the finding reported earlier [21]. As discussed in section 3.2.4, the q_m of activated RS, i.e. acid treated RS, was observed to be as high as $2.12\,\mathrm{mg\,g^{-1}}$. Despite of higher adsorption efficiency of acid treated RS, the raw RS without any treatment has been suggested to be used as the adsorbent, since it does not incur any capital and processing costs. Moreover, phosphate loaded exhausted RS can be used in the agricultural sector as phosphate fertilizer.

Langmuir equation can also be used to calculate a dimensionless equilibrium parameter, R_L also known as the separation factor [38] and can be expressed as:

$$R_L = 1/(1 + bC_0) \tag{6}$$

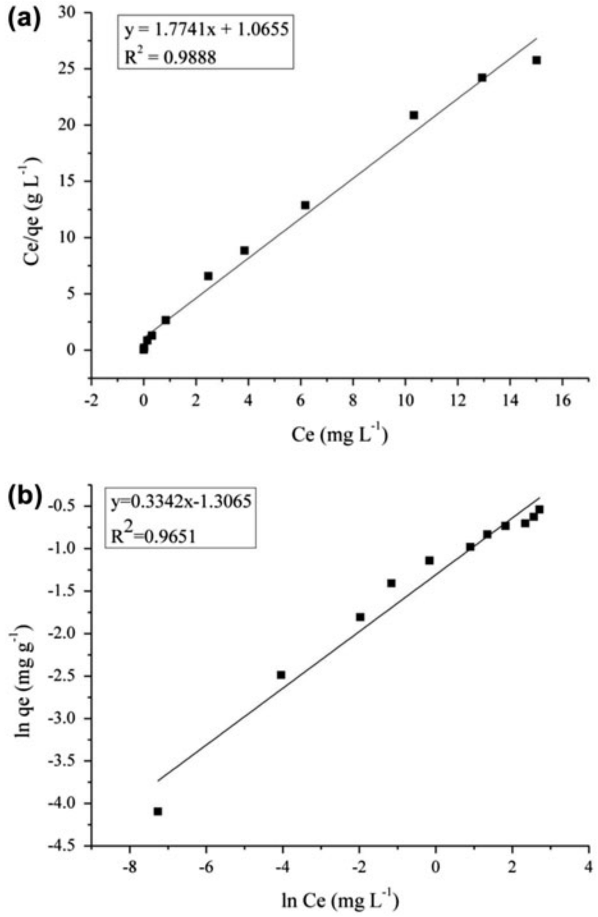

Fig. 10. Adsorption isotherms for phosphate adsorption on RS: (a) Langmuir model and (b) Freundlich model. (Conditions: contact time 90 min, agitation 175 rpm, adsorbent 6 g per 100 mL, adsorbate 1–50 mg $\mathrm{L^{-1}}$, pH 7, and temperature 27 ± 2°C).

Table 3
Parameters of isotherm and kinetics models

Langmuir model	q_m ($\mathrm{mg\,g^{-1}}$)	b ($\mathrm{L\ mg^{-1}}$)	R^2
	0.56	1.67	0.98
Freundlich model	K_f ($\mathrm{mg\,g^{-1}}$)	n	R^2
	0.27	2.99	0.96
Pseudo-first-order model	q_e ($\mathrm{mg\,g^{-1}}$)	k_1 ($\mathrm{min^{-1}}$)	R^2
	0.43	−0.078	0.54
Pseudo-second-order model	q_e ($\mathrm{mg\,g^{-1}}$)	k_2 ($\mathrm{g\ (mg\ min)^{-1}}$)	R^2
	0.35	0.26	0.99

where, C_0 is the initial concentration of phosphate ($\mathrm{mg\,L^{-1}}$).

$R_L = 1$ represents linear adsorption, while $R_L = 0$ stands for the irreversible adsorption process. $R_L < 1$ is for favorable adsorption, while $R_L > 1$ represents unfavorable adsorption. In this case, the value of R_L was found to be 0.03, suggesting that the adsorption process was favorable.

The impulsiveness of the adsorption process can be analyzed based upon the values of Gibbs free energy changes, ΔG°. Langmuir constant, b, is also helpful in finding ΔG° for the adsorption process as per the following equation [45]:

$$\ln\,(1/b) = \Delta G^\circ/(RT) \tag{7}$$

where R is the universal gas constant ($8.314\,\mathrm{J\,mol^{-1}\,K^{-1}}$) and T is the absolute temperature. Based upon Eq. (7), the Gibbs free energy ΔG° observed to be negative ($-1.279\,\mathrm{kJ\,mol^{-1}}$) which necessarily represents the spontaneity of the phosphate adsorption process by RS as an adsorbent.

3.3.2. Freundlich model

The Freundlich isotherm model explains about the adsorption process wherein a heterogeneous adsorbent surface involves in the multilayer distribution of the adsorbate with interaction amongst adsorbed molecules. The linear form of Freundlich isotherm model is given below as Eq. (8) [45]:

$$\ln\,q_e = \ln k_f + (1/n)\ln\,C_e \tag{8}$$

where k_f ($\mathrm{mg\,g^{-1}}$) is the Freundlich constant which represents the adsorption capacity and "n" is the Freundlich exponent that represents the adsorption intensity. k_f is related to temperature and the chemical or physical characteristics of adsorbents, whereas "n" is an indicator of the change of intensity of adsorption process and also a measure of the deviation from linearity of the adsorption. A higher value of n ($n > 1$) indicates favorable adsorption, where as $n < 1$ represents poor adsorption characteristics [37]. In this study, the values of k_f and n (Table 3) were calculated from the intercept and slope of the Freundlich isotherm which is drawn by plotting ln q_e vs. ln C_e (Fig. 10(b)). The value of $n = 2.99$ suggests favorable adsorption.

Isotherm constants of both the models are summarized in Table 3. The correlation coefficient, R^2, values of both the models were higher than 0.96, suggesting that the experimental data demonstrate a very good mathematical fit to both the models and this can be interpreted in terms of surface nature of the adsorbent and affinities of different mineralogical forms present in adsorbent towards phosphate. Though both the models fit well, the R^2 value for Langmuir model (0.98) is marginally higher than that of the Freundlich model (0.96), which may indicate the predominance of monolayer adsorption process over intra-molecular interactions amongst the adsorbed phosphates.

3.4. Adsorption kinetics

The kinetic study of adsorption process is important as it gives insight into the rate of adsorption process, which is helpful in finding out contact time required for adsorption to take place and also facilitates evaluation of reaction coefficients. To investigate the mechanism of adsorption kinetics of phosphate onto RS, two kinetic models, namely pseudo-first-order and pseudo-second-order models were analyzed. The linear forms of pseudo-first-order and pseudo-second-order kinetic models are given below as Eqs. (8) and (9), respectively [3].

$$\log\,(q_e - q_t) = \log q_e - (k_1/2.303)\,t \tag{9}$$

$$t/q_t = 1/(k_2 \cdot {q_e}^2) + (1/q_e)\,t \tag{10}$$

where q_t and q_e ($\mathrm{mg\,g^{-1}}$) are, respectively, the adsorption capacity at any time t and at equilibrium, k_1 is the first-order reaction rate constant ($\mathrm{min^{-1}}$) and k_2 represents the second-order reaction rate constant ($\mathrm{g\,mg^{-1}\,min^{-1}}$). The values of k_1 and q_e were determined from the graph of pseudo-first order model (Fig. 11(a)) that was obtained by plotting log ($q_e - q_t$) vs. t. Similarly, the value of q_e and k_2 for pseudo-second-order model is determined from the slope and intercept of the plot of t/q_t vs. t as shown in Fig. 11(b). The calculated kinetic parameters along with R^2 values for both the kinetic models are given in Table 3. The R^2 value for the pseudo-second-order model (0.99) was much higher than that of the pseudo-first-order model (R^2 = 0.54). Moreover, a very poor correlation between experimentally observed q_e value ($0.32\,\mathrm{mg\,g^{-1}}$) and that the pseudo-first-order kinetic ($0.43\,\mathrm{mg\,g^{-1}}$) was observed with negative reaction constant ($k_1 = -0.078$), indicating the inadequacy of the pseudo-first-order kinetic model. Whereas in case of pseudo-second-order kinetic model, the calculated equilibrium adsorption capacity ($q_e = 0.35\,\mathrm{mg\,g^{-1}}$) was in good agreement with that of the experimentally obtained value ($q_e = 0.32\,\mathrm{mg\,g^{-1}}$). The results

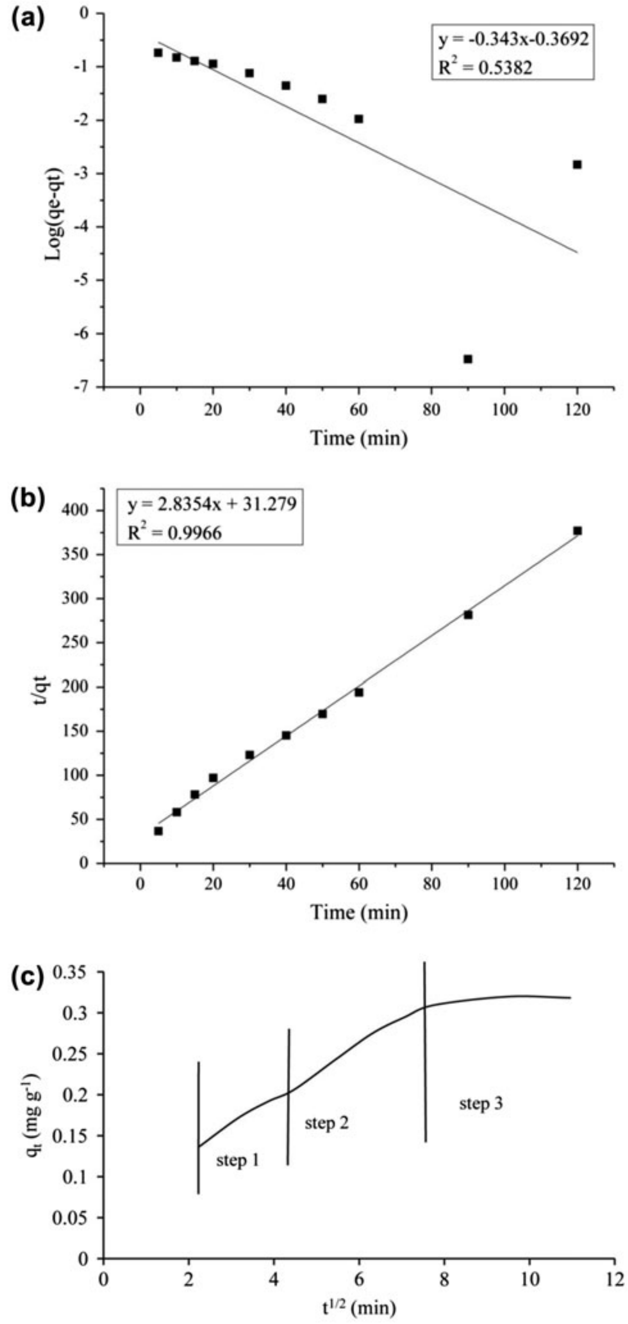

Fig. 11. Kinetic models for phosphate adsorption on RS: (a) Pseudo-first order, (b) pseudo-second order and (c) intra-particle diffusion. (Conditions: contact time 5–120 min, agitation 175 rpm, adsorbent 6 g per 100 mL, adsorbate 20 mg L^{-1}, pH 7, and temperature 27 ± 2˚C).

indicated that the adsorption kinetics of phosphate on RS follows pseudo-second-order kinetics. The best-fit pseudo-second-order kinetics presumes that the rate of adsorption is proportional to the square of the number of unoccupied sites on the adsorbent surface and to the concentration of adsorbate in the solution as well. Thus suggesting that the adsorbates can be bound to different binding sites on the adsorbent. Similar types of findings were also reported by earlier researchers [3,36,38].

Basically, the adsorption process is controlled by the slowest steps of the reaction, i.e. either external mass transfer (film diffusion) or intra-particle diffusion (pore diffusion) or by both. The rate-limiting step of the adsorption process can be predicted by diffusion coefficients calculated from a diffusion model. The presence or absence of intra-particle diffusion can be confirmed by the application of the linear form of the Morris–Weber equation as mentioned below in Eq. (11) [46].

$$q_t = k_p\, t^{1/2} + C \tag{11}$$

where k_p is the intra-particle diffusion rate constant (mg g^{-1} $min^{-1/2}$), q_t (mg g^{-1}) is the phosphate uptake amount at time t (min), and C is the constant indicating the thickness of the boundary layer. Plot of q_t vs. $t^{1/2}$ is shown in Fig. 11(c). The coefficient, k_p, can be determined from the slope and C from the intercept of the plot. Fig. 11(c) shows that the plot of q_t vs. $t^{1/2}$ is not a straight line, indicating that intra-particle diffusion is not the only rate-limiting step. Along with intra-particle diffusion, other mechanisms may also be involved in the adsorption process. The presence of first, second, and third step on the curve is possibly due to the presence of boundary layer diffusion, intra-particle diffusion, and saturation step, respectively. Therefore, both pore diffusion and film diffusion are likely to affect the adsorption process. This supports the earlier discussion (section 3.2.6) about the diffusional nature of the adsorption process.

3.5. Column study

In case of column study, the influent flows continually through the adsorbent bed showing greater similarities to the flow conditions of an actual long-term treatment process. From the practical utility point of view, column study which simulates actual wastewater treatment processes provides more reasonable laboratory results. So, the column study was performed to investigate phosphorus removal efficiency of adsorbent by implementing all the optimized adsorption process parameters obtained from batch study. The flow rate was adjusted to 4.2 mL min^{-1} with the help of peristaltic pumps, in order to maintain the equilibrium contact time for phosphate adsorption, i.e. 90 min. The breakthrough curve as obtained from the column study is illustrated in

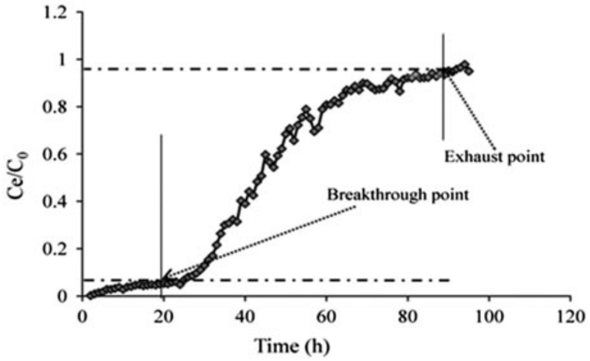

Fig. 12. Breakthrough curve of column study. (Conditions: flow rate 4.2 mL min^{-1}, pH 7, bed height 20 cm, and initial phosphate concentration, C_0, 20 mg L^{-1}).

Fig. 12. The breakthrough time corresponding to 95.33% removal of phosphate, i.e. an effluent phosphate concentration less than 1 mg L^{-1} was found to be 19 h; whereas, exhaust time matching to 5% removal of phosphate was 88 h. The volumes of water treated corresponding to breakthrough time and exhaust time were 4.75 and 22 L, respectively. It took 3.2 h for the exchange zone to be formed initially. The height of the exchange zone was 16.2 cm with a movement rate of 0.23 cm h^{-1}. From the breakthrough curve, the equilibrium adsorption capacity of RS corresponding to breakthrough time was calculated to be 0.30 mg g^{-1}, which is in good agreement with the equilibrium adsorption capacity (0.32 mg g^{-1}) obtained experimentally. The observed minor difference between the batch and column operation may be due to the difference in mode of interaction of adsorbate and adsorbent in the two cases. In batch mode, liquid state predominates and constant agitation may help in proper exposure of binding sites and minimizing the thickness of the mass transfer barrier as well. On the other hand, in column mode solid state predominates. Liquid flow through the adsorbent bed may result in incomplete exhaustion of the adsorbent due to channelization of flow. Thus, the lesser equilibrium capacity compared to batch mode.

3.6. *Effect of coexisting anions*

Common anions such as SO_4^{2-}, NO_3^-, and Cl^- are generally present in wastewater and might show competition to phosphate adsorption onto RS. Typical concentrations of SO_4^{2-}, NO_3^-, and Cl^- in high strength domestic wastewater were found to be 50, 70, and 90 mg L^{-1}, respectively [44]. So the intervention of coexisting anions on phosphate adsorption was evaluated by considering 50 mg L^{-1} of SO_4^{2-}, 70 mg L^{-1} of NO_3^-, and 90 mg L^{-1} of Cl^- ions as model competing anions. Maintaining the phosphate ion concentration as 20 mg L^{-1}, the experiments were carried out at pH 7 and at an adsorbent dose of 6 g per 100 mL. The results given in Table 4 show no significant change in phosphate adsorption onto RS, after adding coexisting anions with concentrations more than that of phosphate ions. This may be attributed to the specific adsorption of phosphate onto the specific active site of the adsorbent, which is not generally influenced by the presence of other ions [43]. The observation demonstrates that RS has high adsorption selectivity towards phosphate. So, RS could remove phosphate effectively even in the presence of coexisting competitive anions, which is advantageous for its potential application as an adsorbent for phosphate removal from real domestic wastewater.

Table 4
Effect of coexisting anions

Concentration of anions (mg L^{-1})				% phosphate removal
PO_4^{3-}	SO_4^{2-}	NO_3^-	Cl–	
20	0	0	0	95.3
20	50	0	0	95.5
20	0	70	0	95.9
20	0	0	90	96.2
20	50	70	90	94.0

3.7. *Treatment of real domestic wastewater*

The applicability of RS as adsorbent was also verified with real domestic wastewater. The characteristics of the domestic wastewater before and after adsorption are given in Table 2. The optimized parameters obtained through the batch and column study of synthetic phosphate solution were adopted for phosphate removal from real domestic wastewater. The concentration of phosphate in the domestic wastewater was very low, 5.62 mg L^{-1}, as compared to the synthetic phosphate solution (20 mg L^{-1}). The batch study with real domestic wastewater revealed that the adsorbent dose of 2.5 g per 100 mL and an equilibrium time were sufficient enough to get an effluent concentration of 0.01 mg L^{-1} of phosphate, resulting in a removal efficiency of. The higher equilibrium time (110 min) of real sample as compared to synthetic sample (90 min) may be explained on the basis of higher removal efficiency of real sample (99.8%) than that of synthetic one (≈96.5%). Since up to equilibrium time, increase in contact time results in increase in removal efficiency [37]. Adsorption data fitted well to Langmuir isotherm

($C_e/q_e = 2.43 + 3.206\ C_e$, $R^2 = 0.904$) with the maximum adsorption capacity (q_m) of 0.311 mg g^{-1}. Experimentally calculated values of R_L = 0.118 and Gibb's free energy change, ΔG° = −0.698 kJ mol^{-1}, suggest the favorability and spontaneity of the process. The column study was performed by pumping domestic wastewater with the help of peristaltic pump at a flow rate of 4.2 mL min^{-1} through the column packed with RS as an adsorbent. The column was operated for a period of 7 days, during which there was no appearance of the exhaustion point. The breakthrough time corresponding to 83% removal of influent concentration was found to be 70 h. In this case, 83% removal (less than 1 mg L^{-1} of effluent phosphate) was opted as the breakthrough point instead of 95.33%, since the initial phosphate concentration was low. During column mode of operation, leaching study was performed to find out the leaching potential of the constituents of adsorbent (Si, Fe, Al, Mg etc.). Even though the adsorbent contains a considerably high amount of Si, Fe, Al, and Mg, insignificant leaching of the components was observed in the treated water. The aluminium leaching was reported to be approximately 0.129 mg L^{-1} followed by iron leaching (0.037 mg L^{-1}) and there was no trace of other constituents of adsorbent found in the effluent of column study. The results of column study revealed that apart from phosphate removal, there was some variations observed in the values of other parameters like TDS, NO_3^--N, NH_4^+-N COD, BOD, DO, etc. The removal of TDS, ammonium ion, COD, and BOD may be a result of effective adsorption onto the RS. However, a minor increase in the value of the DO is possibly due to the passive aeration during percolation of wastewater through the adsorbent bed. Aeration may also result in nitrification of some ammoniacal nitrogen, thereby slight increase in value of nitrate was observed after passing through the adsorbent column [31].

3.8. Desorption study

A good and efficient adsorbent should have a basic property of reusability. It should respond well to process of desorption which is essential for regeneration of the adsorbent. In this study, approximately 6 g of phosphate loaded RS was subjected to desorption in 100 mL of 0.1 M KCl solution agitated at 200 rpm for 24 h (other parameters maintained at the same value as that of adsorption experiment) following slightly modified procedure as described by Ye et al. [47]. The desorbability of phosphate was found to be in the range of 75–80%. Though very high rate of desorption was observed for RS; however considering (i) the local availability of RS, (ii) cost of desorption process, and (iii) applicability of spent RS as phosphate fertilizer, desorption process is not encouraged. However, the desorption followed by reusability of the adsorbent was explored in this study. The desorbed adsorbent was washed several times with distilled water to neutral pH and dried in hot-air oven at 100°C for overnight before using for phosphate adsorption again [48]. In the second time use (maintaining all optimum parameters), the phosphate removal efficiency of the adsorbent was observed to be 67–71% as compared to approximately 96% in the case of first use. The observed lesser efficiency in second use is possibly due to the occupancy of some of the active sites of the adsorbent by the nondesorbed phosphates (since the desorption rate is 75–80%). There is also probability that the number of active sites for adsorption decreases after every use of the adsorbent. The desorption results represent two very important phenomena. Firstly, the adsorption of phosphates on RS is relatively reversible, suggesting the type of adsorption might be a case of physical adsorption as discussed earlier (section 3.2.6). Secondly, the easily desorbed phosphates indicate the availability of labile phosphates for growth of plants, thereby making the application of RS as an eco-friendly and green adsorption technology for the removal of phosphates from domestic wastewater. The spent RS can be applied as soil conditioner and as phosphate fertilizer safely in agricultural uses.

4. Conclusion

The present study evaluates the efficacy of RS as an adsorbent for the removal of phosphates from synthetic as well as real domestic wastewater. In this study, the phosphate adsorption by RS was observed to respond well to both the Langmuir and Freundlich isotherms. Best fit to the pseudo-second-order reaction kinetics indicates that both the concentration of adsorbate as well as adsorbent govern the phosphates adsorption rate by RS. Intra-particle diffusion model suggests the diffusional nature of the adsorption process. Both film diffusion and pore diffusion governs the rate of adsorption of phosphate onto RS. Based upon the experiments, it can be concluded that the application of RS for adsorptive removal of phosphates is highly favorable and a spontaneous process. Therefore, it can be proposed that RS can be used as a low cost and highly efficient natural adsorbent for removal of phosphates from wastewater.

Abbreviations

PIXE — proton induced X- ray emission
PIGE — proton induced γ- ray emission
PAOs — phosphorous accumulating organisms
DPB — denitrifying phosphorous removing bacteria
RS — red soil
RST — red soil treated
ZPC — zero point charge

List of symbols

C_0 — initial phosphate concentrations, mg L^{-1}
C_e — equilibrium phosphate concentrations, mg L^{-1}
q_e — equilibrium uptake capacity of adsorbent, mg g^{-1}
q_t — adsorption capacity at any time t, mg g^{-1}
q_m — maximum adsorption capacity, mg g^{-1}
b — Langmuir adsorption constant, L g^{-1}
V — volume of phosphate solution, mL
m — mass of adsorbent, g
R_L — separation factor
ΔG° — Gibbs free energy changes, kJ mol^{-1}
R — universal gas constant (8.314) J mol^{-1} K^{-1}
T — absolute temperature
k_f — Freundlich constant, mg g^{-1}
n — Freundlich exponent
k_1 — first-order reaction rate constant, min^{-1}
k_2 — second-order reaction rate constant, g mg^{-1} min^{-1}
k_p — intra-particle diffusion rate constant, mg g^{-1} $min^{-1/2}$

Acknowledgments

The authors would like to thank Dr R. Acharya and Mr K. B. Dasari of BARC, Mumbai, Mr D. K. Ray of IOP, Bhubaneswar, and Dr A. Basu of NIT, Rourkela, for their kind help in doing PIGE, PIXE, and XRD experiments and analysis. The authors are also thankful to School of Infrastructure, Indian Institute of Technology, Bhubaneswar, India, for providing facilities to carry out the research work in the concerned area.

References

[1] N. Majed, Y. Li, A.Z. Gu, Advances in techniques for phosphorus analysis in biological sources, Curr. Opin. Biotech. 23 (2012) 852–859.
[2] N. Moelants, I.Y. Smets, J.F. Van Impe, The potential of an iron rich substrate for phosphorus removal in decentralized wastewater treatment systems, Sep. Purif. Technol. 77 (2011) 40–45.
[3] S. Hussain, H.A. Aziz, M.H. Isa, A. Ahmad, J.V. Van Leeuwen, L. Zou, S. Beecham, M. Umar, Orthophosphate removal from domestic wastewater using limestone and granular activated carbon, Desalination 271 (2011) 265–272.
[4] B.A. Hauser, Practical Manual of Wastewater Chemistry, Ann Arbor Press, Chelsea, MI, 1996.
[5] G.W. Vanloon, S.J. Duffy, Environmental Chemistry-a Global Perspective, Oxford University Press, Oxford, 2002.
[6] A.N. Sharpley, H. Tunney, Phosphorus research strategies to meet agricultural and environmental challenges of the 21st century, J. Environ. Qual. 29 (2000) 176–181.
[7] R.H. Kadlec, R.L. Knight, Treatment Wetlands. CRC Press, Boca Raton, 1996.
[8] H.S. Altundogan, F. Tumen, Removal of phosphates from aqueous solutions by using bauxite. I: Effect of pH on the adsorption of various phosphates, J. Chem. Technol. Biotechnol. 77 (2002) 77–85.
[9] Y. Li, C. Liu, Z. Luan, X. Peng, C. Zhu, Z. Chen, Z. Zhang, J. Fan, Z. Jia, Phosphate removal from aqueous solutions using raw and activated red mud and fly ash, J. Hazard. Mater. 137 (2006) 374–383.
[10] D. Mulkerrins, A.D.W. Dobson, E. Colleran, Parameters affecting biological phosphate removal from wastewaters, Environ. Int. 30 (2004) 249–259.
[11] K. Karageorgiou, M. Paschalis, G.N. Anastassakis, Removal of phosphate species from solution by adsorption onto calcite used as natural adsorbent, J. Hazard. Mater. 139 (2007) 447–452.
[12] G. Akay, B. Keskinler, A. Çakici, U. Danis, Phosphate removal from water by red mud using crossflow microfiltration, Water Res. 32 (1998) 717–726.
[13] G.M. Ayoub, B. Koopman, N. Pandya, Iron and aluminum hydroxy (oxide) coated filter media for low-concentration phosphorus removal, Water Environ. Res. 73 (2001) 478–485.
[14] A.O. Babatunde, Y.Q. Zhao, A.M. Burke, M.A. Morris, J.P. Hanrahan, Characterization of aluminium-based water treatment residual for potential phosphorus removal in engineered wetlands, Environ. Pollut. 157 (2009) 2830–2836.
[15] J.P. Gustafsson, A. Renman, G. Renman, K. Poll, Phosphate removal by mineral-based sorbents used in filters for small-scale wastewater treatment, Water Res. 42 (2008) 189–197.
[16] N.M. Agyei, C.A. Strydom, J.H. Potgieter, An investigation of phosphate ion adsorption from aqueous solution by fly ash and slag, Cement Concrete Res. 30 (2000) 823–826.
[17] E. Oguz, Thermodynamic and kinetic investigations of PO_4^{3-} adsorption on blast furnace slag, J. Colloid Interf. Sci. 281 (2005) 62–67.
[18] E.J. Dunne, N. Culleton, G. O'Donovan, R. Harrington, K. Daly, Phosphorous retention and sorption by constructed wetland soils in Southeast Ireland, Water Res. 39 (2005) 4355–4362.
[19] L. Zhang, S. Hong, J. He, F. Gan, Y.S. Ho, Adsorption characteristic studies of phosphorus onto laterite, Desalin. Water Treat. 25 (2011) 98–105.
[20] L. Zhang, W. Wu, J. Liu, Q. Zhou, J. Luo, J. Zhang, X. Wang, Removal of phosphate from water using raw and activated laterite: Batch and column studies, Desalin. Water. Treat. (2013) 1–9, doi: 10.1080/19443994.2013.826786.
[21] H. Liang, J. Liu, Y. Wei, X. Guo, Evaluation of phosphorus removal from wastewater by soils in rural areas in China, J. Environ. Sci. 22 (2010) 15–22.

[22] G.C. Sahu, A. Mishra, Soils of Odisha and its management, Odisha Review 16 (2005) 56–60.

[23] D. Sarkar, Fundamentals and Application of Pedology, Kalyani publisher, Ludhiana, 2006.

[24] APHA, AWWA, WPCF, American Public Health Association, 20th ed., 1999.

[25] V.J. Kennedy, A. Augusthy, K.M. Varier, P. Magudapathy, S. Panchapakesan, K.G.M. Nair, V. Vijayan, Elemental analysis of river sediments by PIXE and PIGE, Int. J. PIXE 9 (1999) 407–416.

[26] P. Faria, J. Órfão, M. Pereira, Adsorption of anionic and cationic dyes on activated carbons with different surface chemistries, Water Res. 38 (2004) 2043–2052.

[27] D.M.R. Mateus, H.J.O. Pinho, Phosphorus removal by expanded clay—six years of pilot-scale constructed wetlands experience, Water Environ. Res. 82 (2010) 128–137.

[28] J. Yang, S. Wang, Z.B. Lu, J. Yang, S.J. Lou, Converter slag–coal cinder columns for the removal of phosphorous and other pollutants, J. Hazard. Mater. 168 (2009) 331–337.

[29] L. Johansson, J.P. Gustafsson, Phosphate removal using blast furnace slags and opoka-mechanisms, Water Res. 34 (2000) 259–265.

[30] W.L. Lindsay, Chemical Equilibria in Soils, Wiley, New York, NY, 1979.

[31] J.G. Chen, H.N. Kong, D.Y. Wu, X.C. Chen, D.L. Zhang, Z.H. Sun, Phosphate immobilization from aqueous solution by fly ashes in relation to their composition, J. Hazard. Mater. 139 (2007) 293–300.

[32] J.M. Chimenos, A.I. Fernández, G. Villalba, M. Segarra, A. Urruticoechea, B. Artaza, F. Espiell, Removal of ammonium and phosphates from wastewater resulting from the process of cochineal extraction using MgO-containing by-product, Water Res. 37 (2003) 1601–1607.

[33] T.T. Zheng, Z.X. Sun, X.F. Yang, A. Holmgren, Sorption of phosphate onto mesoporous γ-alumina studied with *in situ* ATR-FTIR spectroscopy, Chemistry Cent. J. 6 (2012) 26–36.

[34] E.J. Elzinga, D.L. Sparks, Phosphate adsorption onto hematite: An *in situ* ATR-FTIR investigation of the effects of pH and loading level on the mode of phosphate surface complexation, J. Colloid Interf. Sci. 308 (2007) 53–70.

[35] E.W. Shin, J. Han, Phosphate adsorption on aluminum-impregnated mesoporous silicates: Surface structure and behavior of adsorbents, Environ. Sci. Technol. 38 (2004) 912–917.

[36] K.A. Krishnan, A. Haridas, Removal of phosphate from aqueous solutions and sewage using natural and surface modified coir pith, J. Hazard. Mater. 152 (2008) 527–535.

[37] S. Yang, Y. Zhao, R. Chen, C. Feng, Z. Zhang, Z. Lei, Y. Yang, A novel tablet porous material developed as adsorbent for phosphate removal and recycling, J. Colloid Interf. Sci. 396 (2013) 197–204.

[38] A.M. Baraka, M.M. El-tayieb, M.El. Shafai, N.Y. Mohamed, Sorptive removal of phosphate from wastewater using activated red mud. Aust. J. Basic & Appl. Sci. 10 (2012) 500–510.

[39] P. Pengthamkeerati, T. Satapanajaru, P. Chularuengoaksorn, Chemical modification of coal fly ash for the removal of phosphate from aqueous solution, Fuel 87 (2008) 2469–2476.

[40] D.C. Harris, Quantitative Chemical Analysis, W.H. Freeman Company, New York, NY, 1987.

[41] C.G. Lee, J.A. Park, S.B. Kim, Phosphate removal from aqueous solutions using slag microspheres, Desalin. Water. Treat. 44 (2012) 229–236.

[42] A. Elnemr, Phosphate Removal from Aqueous Solutions by Adsorption onto Ammonium- functionalized Mesoporous Silica, MSc Thesis, Department of Soil and Agricultural Engineering, University of Laval, Qebec, 2009.

[43] Y.S. Chen, W.C. Chang, S.M. Chiang, C.C. Tseng, M.H. Su, Reusing spent polyaluminum chloride sludge as adsorbent for phosphate removal from secondary wastewater effluent, Desalin. Water. Treat. 51 (2013) 3344–3352.

[44] Metcalf and Eddy Inc., Wastewater Engineering: Treatment, Disposal and Reuse, McGraw-Hill Co., New York, NY, 2003.

[45] S.K. Maji, A. Pal, T. Pal, Arsenic removal from real-life groundwater by adsorption on laterite soil, J. Hazard. Mater. 151 (2008) 811–820.

[46] W.T. Chen, C.W. Lin, P.K. Shih, W.L. Chang, Adsorption of phosphate into waste oyster shell: Thermodynamic parameters and reaction kinetics, Desalin. Water. Treat. 47 (2012) 86–95.

[47] H. Ye, F. Chen, Y. Sheng, G. Sheng, J. Fu, Adsorption of phosphate from aqueous solution onto modified palygorskites, Sep. Purif. Technol. 50 (2006) 283–290.

[48] S.K. Maji, S.W. Wang, C.W. Liu, Arsenate removal from aqueous media on iron-oxidecoated natural rock (IOCNR): A comprehensive batch study, Desalin. Water. Treat. 51 (2013) 7775–7790.